

## Exact Floquet states of a two-component Bose–Einstein condensate induced by a laser standing wave

This article has been downloaded from IOPscience. Please scroll down to see the full text article.

2006 J. Phys. A: Math. Gen. 39 15061

(<http://iopscience.iop.org/0305-4470/39/49/001>)

View [the table of contents for this issue](#), or go to the [journal homepage](#) for more

Download details:

IP Address: 171.66.16.108

The article was downloaded on 03/06/2010 at 04:58

Please note that [terms and conditions apply](#).

# Exact Floquet states of a two-component Bose–Einstein condensate induced by a laser standing wave

Haiming Deng, Wenhua Hai and Qianquan Zhu

Department of Physics, Hunan Normal University, Changsha 410081, People's Republic of China

E-mail: [whhai2005@yahoo.com.cn](mailto:whhai2005@yahoo.com.cn)

Received 21 July 2006, in final form 27 October 2006

Published 21 November 2006

Online at [stacks.iop.org/JPhysA/39/15061](http://stacks.iop.org/JPhysA/39/15061)

## Abstract

Based on the idea of balance between the internal and external potentials, it is shown that for a two-component Bose–Einstein condensate (BEC) confined in an optical lattice the presence of a spacetime periodic laser field can induce a family of exact Floquet states (EFSs). The atomic-number densities of the EFSs are illustrated and the atomic current, phase blowing-up and the quantum reflection are investigated. The balance conditions and blowing-up region on parameter space are found, and the influences of phase blowing-up to the velocity fields, flow densities are revealed. It is demonstrated that the BEC motions can be controlled by adjusting the laser frequency, wave vector and amplitude.

PACS numbers: 03.75.Lm, 03.75.Mn, 05.70.Jk, 03.75.Kk

## 1. Introduction

In the mean-field theory, the macroscopic wavefunction of a Bose–Einstein condensate (BEC) obeys Gross–Pitaevskii equation (GPE) [1]. To investigate the physical properties of BEC, we require to seek exact or approximate solutions of GPE. However, the multi-dimensional GPE is not easy to solve in general, because of the combination of the nonlinear interatomic interactions and external fields. Fortunately, the GPE can be reduced to lower dimensional (1D or 2D or (1+1)D) nonlinear Schrödinger equation by one or two strong trapping potentials [2, 3]. Several exact stationary solutions of GPEs have been obtained for the BECs held in the quasi-1D Kronig–Penney potential [4], optical lattices [5–7] and the 2D lattice potentials [8, 9]. By using the exact solutions, many physical properties, such as the stabilities of BEC [5, 6, 10, 11], phase coherence, superfluid velocity and flow density [12], and the generation of soliton [10] are revealed.

In contrast with the stationary state case, there exist few reports in the exact nonstationary solutions of BECs in (1+1)D spacetime dimensions, since their derivations are more difficult compared to the former. Only under some rigorous conditions on the interaction intensities, several exact nonstationary solutions were constructed for an expulsive parabolic potential [13, 14] and for an optical lattice potential [15]. These exact nonstationary solutions described the compression of matter waves, dynamics of bright soliton, stability of solution and the sublattice oscillation of condensates.

The Floquet states are a kind of important nonstationary ones, which have been widely used to research various physical systems, such as the coherent states of driven Rydberg atom [16], chaotic quantum ratchets [17], electron transmission in semiconductor heterostructures [18], selectively suppressing of tunnelling in quantum-dot array [19] and the ionization suppressors of electron [20]. The Floquet states have also been found in BEC systems and been applied to probe superfluid–insulator transition [21], towards coherent control [22] and dynamical tunnelling [23]. It is well known that the GPE with spatially periodic potential has Bloch solution, and it possesses Floquet solution in the presence of time periodic potential. This hints broadly that one can use a spacetime periodic laser field to induce the exact Floquet states (EFSs).

In this paper, we consider a two-component BEC confined in an optical lattice  $V_0 \sin^2 kx$  with strength  $V_0$  and wave vector  $k$ , and seek the interesting EFS by adding a spacetime periodic laser standing wave  $V_1 \cos kx \cos(\omega t - \beta)$ , where  $V_1$ ,  $\omega$  and  $\beta$  denote the laser strength, frequency and initial phase, respectively. In the previous work on the exact solutions of BEC systems, the idea of balance is employed, where the external potential and interatomic interaction reach an indifferent equilibrium at any spatial point [7–9, 12]. For the considered time-dependent BEC system we shall establish a new balance condition at any spatiotemporal point, which leads to a set of EFSs. The spacetime periodical atomic-number densities of the EFSs are illustrated and the properties of the atomic flow, phase blowing-up [24, 25] and the quantum reflection are investigated. We show the parameter region, where the balance solutions exist and the blowing-up region is contained. We also find the spacetime singular points of velocity fields, which are the zero points of atomic-number densities. Effects of the phase blowing-up to the physics of the system are revealed. Finally, it is demonstrated that the velocity fields and flow densities periodically oscillate with the laser frequency and amplitude such that we can control them by adjusting the frequency and amplitude.

The paper is organized as follows. In section 2, we show in detail the construction of exact Floquet states by using the balance condition and illustrate the spacetime evolutions of atomic-number densities. In section 3, we investigate the phase blowing-up, velocity fields and flow densities. Finally, the results are summarized and the corresponding discussions are given in section 4.

## 2. Exact Floquet states

We consider a quasi-1D BEC consisted of  $N = N_1 + N_2$   $^{87}\text{Rb}$  atoms in two coupling hyperfine states,  $|1\rangle = |F = 1, m_F = -1\rangle$  and  $|2\rangle = |F = 2, m_F = 1\rangle$ , where the three-body interaction has been neglected such that the number of atoms  $N_i$  in  $i$  state is a constant. The coupled GPEs governing the BEC read [7]

$$i\hbar \frac{\partial \psi_1}{\partial t} = -\frac{\hbar^2}{2m} \frac{\partial^2 \psi_1}{\partial x^2} + (g_1 |\psi_1|^2 + g_3 |\psi_2|^2) \psi_1 + V(x, t) \psi_1, \quad (1)$$

$$i\hbar \frac{\partial \psi_2}{\partial t} = -\frac{\hbar^2}{2m} \frac{\partial^2 \psi_2}{\partial x^2} + (g_2 |\psi_2|^2 + g_3 |\psi_1|^2) \psi_2 + V(x, t) \psi_2. \quad (2)$$

Here,  $m$  is the atomic mass of  $^{87}\text{Rb}$ ;  $g_i = 2\hbar\omega_r a_{si}$ , for  $i = 1, 2, 3$  [26], represent the interaction intensities with  $g_{1,2}$  being the interaction intensities between the atoms in component 1 or 2 and  $g_3$  is the interaction intensity between the two different components,  $a_{si}$  is the corresponding s-wave scattering length,  $\omega_r$  is the radial trap frequency and is evaluated as  $\omega_r = 2\pi \times 700$  Hz hereafter. In the presence of the spacetime periodic laser field the external potential is of the form

$$V(x, t) = V_0 \sin^2 kx + V_1 \cos kx \cos(\omega t - \beta). \quad (3)$$

The first term is a normal optical-lattice potential and the second term denotes a time-periodically modulated optical standing wave, both with the same wavelength  $\lambda = 2\pi/k$ .

When the external optical potential and the internal interaction potentials experimentally reach into an indifferent equilibrium, we establish the balance condition, namely the sum of the external potential and any set of the internal potentials equates a constant [7]. Setting the constant as  $\mu$  which is the chemical potential of the system yields

$$(g_1 |\psi_1|^2 + g_3 |\psi_2|^2) + V = \mu, \quad (4)$$

$$(g_2 |\psi_2|^2 + g_3 |\psi_1|^2) + V = \mu. \quad (5)$$

Then equations (1) and (2) are reduced to the linear Schrödinger equations with constant potential  $\mu$ :

$$i\hbar \frac{\partial \psi_j}{\partial t} = -\frac{\hbar^2}{2m} \frac{\partial^2 \psi_j}{\partial x^2} + \mu \psi_j, \quad \text{for } j = 1, 2. \quad (6)$$

The balance conditions (4) and (5) fix the amplitudes of the wavefunction  $\psi_j$ , and the Schrödinger equation (6) not only give the same amplitudes but also describe the phases of wavefunctions [7].

Solving equations (4) and (5) for the atomic-number densities, we get

$$|\psi_j|^2 = G_j (\mu - V), \quad \text{for } j = 1, 2, \quad (7)$$

where  $G_1 = \frac{g_3 - g_2}{g_3^2 - g_1 g_2}$ ,  $G_2 = \frac{g_3 - g_1}{g_3^2 - g_1 g_2}$ . Integrating the atomic-number densities in a single period of potential, we get the atomic numbers  $N'_1, N'_2$  of the two components per spatial-period as

$$\int_{2l\pi/k}^{2(l+1)\pi/k} |\psi_j|^2 dx = \frac{2\pi}{k} \cdot G_j \left( \mu - \frac{V_0}{2} \right) = N'_j, \quad \text{for } j = 1, 2, \quad (8)$$

where  $l$  is an arbitrary integer. It is interesting to note that the atomic numbers per well are time independent although the number densities of atoms are periodic functions of time. The above two equations imply that the chemical potential can be expressed by the experiment parameters  $N'_j, g_j$  and  $V_0$  as

$$\mu = \frac{kN'_1}{2\pi G_1} + \frac{V_0}{2} = \frac{kN'_2}{2\pi G_2} + \frac{V_0}{2}, \quad (9)$$

and the atomic numbers per well must obey the relation

$$\frac{N'_1}{N'_2} = \frac{G_1}{G_2} = \frac{g_3 - g_2}{g_3 - g_1} = \frac{a_{s3} - a_{s2}}{a_{s3} - a_{s1}}. \quad (10)$$

This is the first condition for the balance solutions in equations (4) and (5), which gives a limitation to the atomic numbers per well and interaction strengths. This condition is weaker than the corresponding condition in [15], where  $a_{s1} = a_{s2} = a_{s3}$  is assumed such that  $N'_1 = N'_2$ .

Substituting equations (3) and (9) into equation (7) gives the atomic-number densities in terms of experimental parameters:

$$|\psi_j|^2 = \frac{G_j(V_c - V_0)}{2} + G_j V_0 \cos^2 kx - G_j V_1 \cos kx \cos(\omega t - \beta), \quad \text{for } j = 1, 2. \quad (11)$$

Here, we have set  $V_c = \frac{kN'_1}{\pi G_1} = \frac{kN'_2}{\pi G_2}$ . From  $|\psi_j|^2 \geq 0$  at  $\cos kx = 0$  we know that  $|V_c|$  is a supercritical value of the potential strength  $|V_0|$ , namely

$$0 < V_0 \leq V_c \quad \text{for } G_j > 0, \quad (12)$$

$$V_c \leq V_0 < 0 \quad \text{for } G_j < 0, \quad (13)$$

so that  $|V_0| \leq |V_c|$ .

Now we solve the linear Schrödinger equation (6) for the Floquet solutions of equations (1) and (2). Equation (6) is so simple that its Floquet solutions can be easily found in the form

$$\psi_j = [(a_j + ib_j) + (c_j + id_j) \cos kx e^{-i(\omega t - \beta)}] \cdot e^{-i\frac{\mu}{\hbar}t} \quad (j = 1, 2), \quad (14)$$

where Floquet energy  $\mu$  is just the chemical potential,  $a_j$ ,  $b_j$ ,  $c_j$  and  $d_j$  are real undetermined constants. Inserting the Floquet solutions into equation (6) gives the second condition of balance solutions as

$$\omega = \frac{\hbar k^2}{2m}, \quad (15)$$

which confines the laser frequency and wave vector. In the calculations of this paper, we evaluate the wave vector  $k = 0.79 \times 10^7 \text{ m}^{-1}$ , so that the values of frequency and recoil energy read  $\omega = 2.30 \times 10^4 \text{ Hz}$  and  $E_R = \hbar\omega = 2.43 \times 10^{-30} \text{ J}$ .

Rewriting the wavefunction in the exponential form

$$\psi_j = R_j(x, t) e^{i\Theta_j(x, t)}, \quad j = 1, 2, \quad (16)$$

we have the norm and phase

$$\begin{aligned} R_j^2(x, t) &= |\psi_j|^2 \\ &= \{a_j + [c_j \cos(\omega t - \beta) + d_j \sin(\omega t - \beta)] \cos kx\}^2 \\ &\quad + \{b_j - [c_j \sin(\omega t - \beta) - d_j \cos(\omega t - \beta)] \cos kx\}^2 \\ &= (a_j^2 + b_j^2) + (c_j^2 + d_j^2) \cos^2 kx + 2[(a_j c_j + b_j d_j) \cos(\omega t - \beta) \\ &\quad + 2(a_j d_j - b_j c_j) \sin(\omega t - \beta)] \cos kx, \end{aligned} \quad (17)$$

$$\Theta_j(x, t) = \arctan \frac{b_j - c_j \cos kx \sin(\omega t - \beta) + d_j \cos kx \cos(\omega t - \beta)}{a_j + c_j \cos kx \cos(\omega t - \beta) + d_j \cos kx \sin(\omega t - \beta)} - \frac{\mu}{\hbar}t. \quad (18)$$

As shown in equation (17), the norm  $R_j^2(x, t)$  is the sum of the squares of real and imaginary parts of  $\psi_j$ , so  $R_j^2(x, t) \geq 0$ . Comparing equation (11) with equation (17), we obtain a set of algebraical equations for  $a_j$ ,  $b_j$ ,  $c_j$  and  $d_j$  as

$$a_j^2 + b_j^2 = \frac{G_j}{2}(V_c - V_0), \quad (19)$$

$$2(a_j c_j + b_j d_j) = -G_j V_1, \quad (20)$$

$$c_j^2 + d_j^2 = G_j V_0, \quad (21)$$

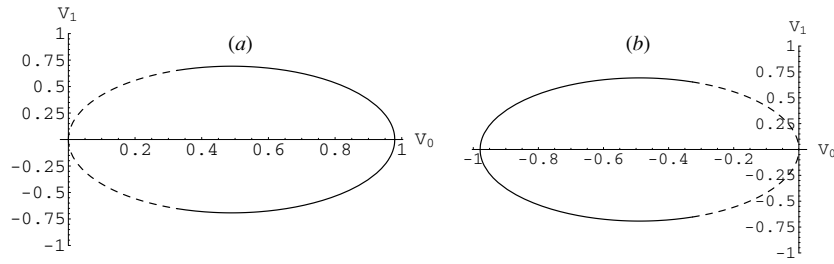


**Figure 1.** The balance region on parameter plane of  $V_1$  versus  $V_0$  for  $N'_1 = 1.4 \times 10^2$  and (a)  $a_{s1} = 4.5$  nm,  $a_{s2} = 3.5$  nm,  $a_{s3} = 5.5$  nm,  $G_1 = 1.479 \times 10^{38}$  (J m) $^{-1}$ ,  $V_c = 2.38 \times 10^{-30}$  J =  $0.979E_R$ ; (b)  $a_{s1} = -4.5$  nm,  $a_{s2} = -3.5$  nm,  $a_{s3} = -5.5$  nm,  $G_1 = -1.479 \times 10^{38}$  (J m) $^{-1}$ ,  $V_c = -2.38 \times 10^{-30}$  J =  $-0.979E_R$ . The solid curves are associated with  $|V_0| \geq |V_c|/3$  and the dashed curves with  $|V_0| < |V_c|/3$ .  $V_1$  and  $V_0$  are in units of recoil energy  $E_R$ .

$$a_j d_j - b_j c_j = 0. \quad (22)$$

From equation (21) we can see  $G_i V_0 > 0$ . This infers that  $G_1$  and  $G_2$  have the same sign. Noticing the definition  $G_i = (g_3 - g_j)/(g_3^2 - g_1 g_2)$  for  $i, j = 1, 2; i \neq j$ , the same sign of  $(g_3 - g_j)$  implies

$$g_3 > g_j \quad \text{or} \quad g_3 < g_j \quad \text{for} \quad j = 1, 2. \quad (23)$$

These two relations can be realized experimentally [27, 28]. In fact, as we known, s-wave scattering length and then the interaction strength can be modified by means of Feshbach resonance [29].

Solving the set of equations (19)–(22), we find that  $a_j, b_j, c_j, d_j$  have real solutions only if

$$V_1 = \pm \sqrt{2V_0(V_c - V_0)}. \quad (24)$$

Combining equations (12) and (13) with equation (24) gives the balance region in parameter space, which is illustrated for given  $V_c$  as in figure 1. In order to induce the possible Floquet state with the form of equation (14), equations (15) and (24) tell us how to chose the strength  $V_1$  and frequency  $\omega$  of the laser standing wave. Because equations (19)–(22) are a set of indefinite algebraical equations, they have an infinite number of solutions. Any set of solutions corresponds to the same amplitudes as in equations (11) and the different phases of equation (18). A set of simplest solutions is

$$b_j = d_j = 0, \quad a_j = \pm \sqrt{\frac{G_j}{2}(V_c - V_0)}, \quad c_j = \pm \sqrt{G_j V_0} \quad (25)$$

that leads equation (14) to the Floquet wavefunction,

$$\psi_j = \left[ \pm \sqrt{\frac{G_j}{2}(V_c - V_0)} \pm \sqrt{G_j V_0} \cos kx e^{-i(\omega t - \beta)} \right] \cdot e^{-i\frac{\hbar}{\hbar} t}, \quad (26)$$

whose amplitudes are same with equation (11).

In the states of equation (26), the atomic numbers of the two BEC components in a spatial period of potential  $V$  are given by equation (8) as  $N'_1$  and  $N'_2$ , respectively, which never change with time. However, the atomic-number densities will periodically evolve, because of the periodicity of the states. From equation (11) we plot the spatiotemporal evolutions of atomic-number density  $|\psi_1|^2$  for several different parameter sets as in figures 2–4. As a reference

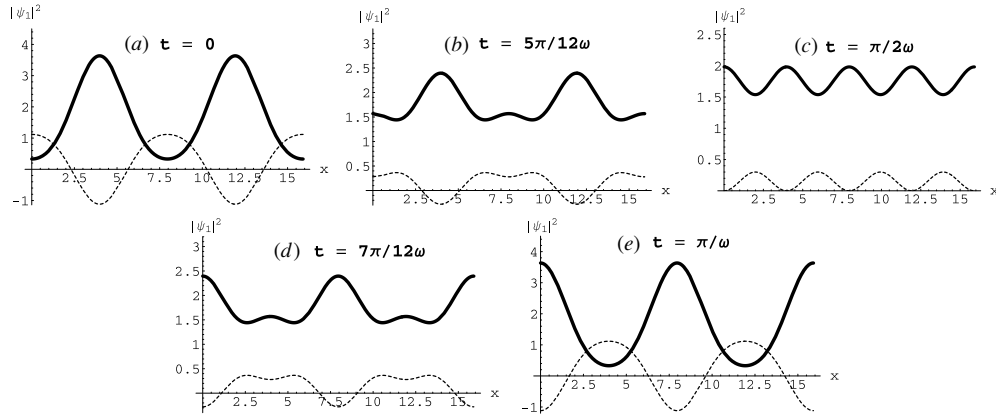


**Figure 2.** The spatial evolutions of the atomic-number density  $|\psi_1|^2$  (solid curves) for  $G_1 = 1.479 \times 10^{38} \text{ (J m)}^{-1}$ ,  $V_c = 0.979 E_R$ ,  $V_0 = 0.123 E_R < V_c/3$ ,  $\beta = 0$ ,  $k = 0.79 \times 10^7 \text{ m}^{-1}$  and  $\omega = 2.30 \times 10^4 \text{ Hz}$  at (a)  $t = 0$ , (b)  $t = \frac{5\pi}{12\omega}$ , (c)  $t = \frac{\pi}{2\omega}$ , (d)  $t = \frac{7\pi}{12\omega}$  and (e)  $t = \frac{\pi}{\omega}$ . The atomic-number density is greater than zero at any spatial position and its maxima fall always to the centres of the potential wells. In figures 2(a) and (e), there is only one density peak in a period of  $V$ , and in figures 2(b)–(d) there are two density peaks in a period of  $V$ . The number density  $|\psi_1|^2$  is normalized in units of  $10^8 \text{ m}^{-1}$  and  $x$  in units of  $10^{-7} \text{ m}$ . The dashed curves denote the potential function, which is in unit of  $10^{-30} \text{ J}$ .

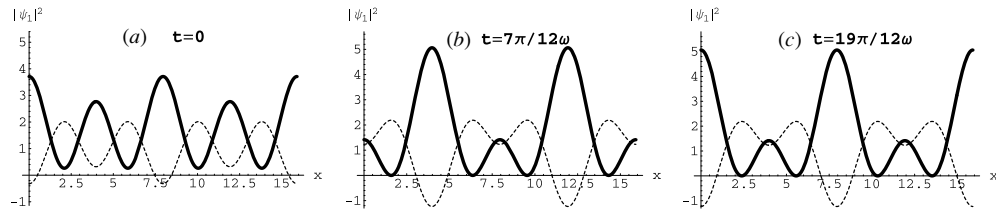


**Figure 3.** The spatial evolutions of the atomic-number density  $|\psi_1|^2$  (solid curves) for  $V_0 = 0.823 E_R > V_c/3$ ,  $\beta = 7\pi/17$  and at (a)  $t = 0$ , (b)  $t = \frac{7\pi}{12\omega}$ , (c)  $t = \frac{19\pi}{12\omega}$ . The other parameters are the same with figure 2. In figure 3(b) and (c), the number density becomes zero at the sites of potential barriers. The dashed curves denote the potential function, which show two subwells in a period of  $V$ . The same units with figure 2 are adopted.

frame, the potential function is plotted in these figures as the dashed curves. The plots of  $|\psi_2|^2$  in equation (11) are similar, so we do not show them here. It is clear in equation (3) that at any moment the potential is spatially periodic and its minima are related to the centres of potential wells. With the increase of time, the depths and positions of potential wells may vary. In figures 2 and 3, we show that when  $G_j > 0$ ,  $V_0 > 0$  are set, although the atomic-number densities have different spatial distributions at different times from zero to a half time-period  $\pi/\omega$  of the potential, their maxima fall always to the centre points of the potential wells. This means that more atoms are distributed to the centres of potential wells compared to that of the potential barrier sites. Such atomic distributions correspond to more stabilities of the BEC system. An important result is numerically found that the atomic-number density is greater than zero at any spatial position for  $G_j > 0$ ,  $V_0 < V_c/3$  as in figure 2, and it may be zero at the peak sites of potential for  $G_j > 0$ ,  $V_0 > V_c/3$  as in figure 3. Mathematically, when a solution of a wave equation or its first derivative equates infinity at a finite time, the solution

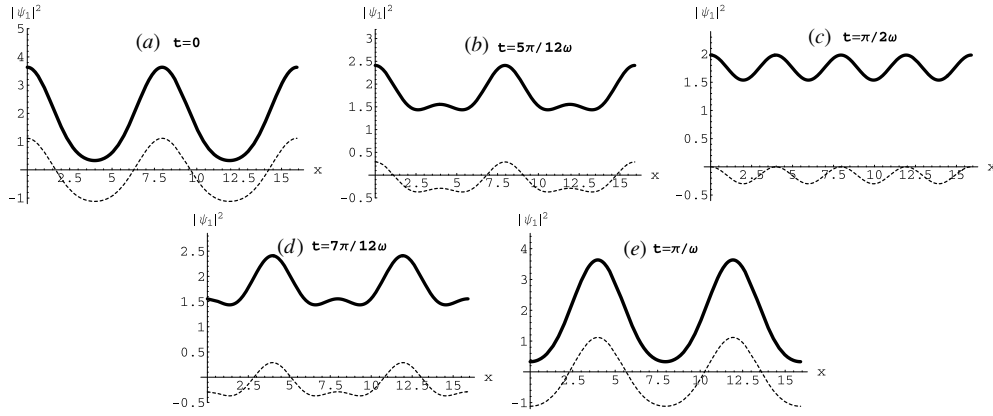


**Figure 4.** The spatial evolution of the atomic-number density  $|\psi_1|^2$  (solid curves) for  $G_1 = -1.479 \times 10^{38} \text{ (J m)}^{-1}$ ,  $V_c = -0.979E_R$ ,  $V_0 = -0.123E_R$  and  $\beta = 0$  at times (a)  $t = 0$ , (b)  $t = \frac{5\pi}{12\omega}$ , (c)  $t = \frac{\pi}{2\omega}$ , (d)  $t = \frac{7\pi}{12\omega}$ , (e)  $t = \frac{\pi}{\omega}$ . The parameters  $\omega$  and  $k$  are the same with figure 2. The maxima of atomic-number density appear always at the peak points of the potential. The dashed curves denote the potential function. The same units are adopted as in figure 2.

is called the blowing-up solution [30]. The zero number density may be associated with an infinite phase gradient, which will be considered as the phase blowing-up in the next section.

Differing from the case  $G_j > 0$ ,  $V_0 > 0$ , when  $G_j < 0$ ,  $V_0 < 0$  are taken, the maxima of atomic-number density appear always at the peaks of the potential, which is exhibited as in figure 4. In such a case, the BEC system may be more unstable. Therefore,  $G_j < 0$ ,  $V_0 < 0$  may be an instability region of the parameter space, which can be avoided for stabilizing the BEC system.

### 3. Atomic flow and phase blowing-up

In the preceding section, we have analytically constructed the exact Floquet solution of the considered system and numerically illustrated its spatiotemporal evolutions. Given the system parameters, the Floquet energy  $\mu$  and the module of solution are completely determined by equation (9) and the balance conditions (4) and (5). The Floquet energy is simply proportional to the laser wave vector  $k$  and strength  $V_0$ , and the module of solution contains the rich motion properties as shown in figures 2–4. Since the phase of our Floquet state is independent of the balance conditions, there are many different selections of phases for a given module. We have only considered the simplest case of equation (25), where the undetermined constants in phase (18) obey  $b_j = d_j = 0$ . We will see that the simplest phase can also play an important role in the exact Floquet state and its applications.

According to the definitions of flow velocity field  $v_j(x, t)$  and current density  $J_j(x, t)$ ,  $v_j(x, t) = \hbar \Theta_{jx} / m$ ,  $J_j(x, t) = R_j^2 v_j$ , both depend on the gradient of phase. Making use of equations (18), (24) and (25), we calculate the phase gradient as

$$\Theta_{jx}(x, t) = \frac{(a_j c_j + b_j d_j) k \sin kx \sin(\omega t - \beta)}{R_j^2(x, t)} = -\frac{G_j V_1 k \sin kx \sin(\omega t - \beta)}{2R_j^2(x, t)}. \quad (27)$$

Although here the simple case with  $b_j = d_j = 0$  of equation (25) has been considered, equation (27) shows that in the general case  $b_j d_j \neq 0$ , the phase gradient varies only the amplitude compared to the former. Applying equation (27) to the definitions of flow velocity



and density results in

$$J_j(x, t) = -\frac{\hbar k G_j V_1 \sin kx \sin(\omega t - \beta)}{2m}, \quad v_j(x, t) = -\frac{\hbar k G_j V_1 \sin kx \sin(\omega t - \beta)}{2m R_j^2(x, t)}. \quad (28)$$

The phase gradient and velocity field are inverse proportional to the atomic-number density. Our interest is thereby what will happen at  $R_j^2(x, t) = 0$  and whether some quantities will become infinity or not in this case? In order to evidence them, we at first extract the spacetime points  $(x_b, t_b)$  at which the value of  $R_j^2(x, t)$  vanishes, and then apply them to the phase gradient and velocity field.

Setting  $|\psi_j(x_b, t_b)|^2 = R_j^2(x_b, t_b) = 0$  in equation (11) and solving it for  $\cos kx_b$ , we get

$$\cos kx_b = \frac{G_1 V_1 \cos(\omega t_b - \beta) \pm \sqrt{G_1^2 V_1^2 [\cos^2(\omega t_b - \beta) - 1]}}{2G_1 V_0}. \quad (29)$$

In the calculation, equation (24) has been employed. In equation (29),  $\cos kx_b$  should be some real numbers that implies  $\cos(\omega t_b - \beta) = \pm 1$ . We shall define  $\cos(\omega t_{b1} - \beta) = 1$  and  $\cos(\omega t_{b2} - \beta) = -1$  such that  $t_{b1} = (2n\pi + \beta)/\omega$  and  $t_{b2} = [(2n + 1)\pi + \beta]/\omega$  for  $n = 0, 1, 2, \dots$ . Inserting them into equation (29) respectively, we obtain two values of  $x_b$ , which obey the definitions  $\cos kx_{b1} = |\frac{V_1}{2V_0}|$  and  $\cos kx_{b2} = -|\frac{V_1}{2V_0}|$ . The number densities vanish only if the spacetime points  $(x_{b\mu}, t_{b\nu})$  for  $\mu, \nu = 1, 2$  satisfy equation (29), otherwise  $R_j^2 > 0$ . Given the definitions of  $(x_{b\mu}, t_{b\nu})$ , inserting them into equation (11) we arrive at

$$R_j^2(x_{b\mu}, t_{b\mu}) = 0, \quad \mu = 1, 2 \quad \text{for } G_1 V_1 > 0, \quad (30)$$

$$R_j^2(x_{b\mu}, t_{b\nu}) = 0, \quad \mu, \nu = 1, 2; \quad \mu \neq \nu, \quad \text{for } G_1 V_1 < 0. \quad (31)$$

Obviously, the inequality  $|\cos kx_{b\mu}| = |\frac{V_1}{2V_0}| \leq 1$  implies the parameter region  $|V_1| \leq 2|V_0|$  in which there exist the zero points  $(x_{b\mu}, t_{b\nu})$  of the atomic-number densities. This region has been indicated by the solid curves in figure 1. Combining this with equation (24), we find three different cases, where the gradients of phase  $\Theta_{jx}(x, t)$  show different characters, respectively.

*Case 1.* In the parameter region  $|V_1| > 2|V_0|$  for  $0 < |V_0| < |\frac{V_c}{3}|$  in equation (24) and as indicated by the dashed curves in figure 1,  $R_j^2(x, t) > 0$  is kept as showed in figures 2 and 4. So  $\Theta_{jx}(x, t)$  and  $v_j(x, t)$  are periodic and always finite in such a case.

*Case 2.* At  $|V_1| = |2V_0|$  for  $V_0 = \frac{V_c}{3}$  in equation (24), we have  $\cos kx_b = \pm |\frac{V_1}{2V_0}| = \pm 1$  and  $\cos(\omega t_b - \beta) = \pm 1$  so that  $\sin(\omega t_b - \beta) = 0$  and  $\sin kx_b = 0$ . Substituting them into equations (27) and (28) leads to  $\Theta_{jx}(x_b, t_b) = 0$ ,  $v_j(x_b, t_b) = 0$  although  $R^2(x_b, t_b) = 0$  in their denominators. And at other spacetime points  $\Theta_{jx}(x, t)$  and  $v_j(x, t)$  are finite, because of  $R_j^2(x, t) > 0$  here.

*Case 3.* In the parameter region  $|V_1| < 2|V_0|$  for  $|\frac{V_c}{3}| < |V_0| < |V_c|$  in equation (24) and as indicated by the solid curves in figure 1,  $\Theta_{jx}(x, t)$  and  $v_j(x, t)$  may tend to infinity at spacetime points  $(x_{b\mu}, t_{b\nu})$ , where  $R^2(x_b, t_b) = 0$  as in figures 3(b) and (c). We call this singularity of phase gradient at a finite time the phase blowing-up, and the region  $|V_1| < 2|V_0|$  is the blowing-up region.

Combining the three cases we know that when  $V_c$  is fixed, the values  $(|V_0|, |V_1|) = (|V_c/3|, |2V_c/3|)$  indicate a bifurcation point for the phase blowing-up on the parameter space.

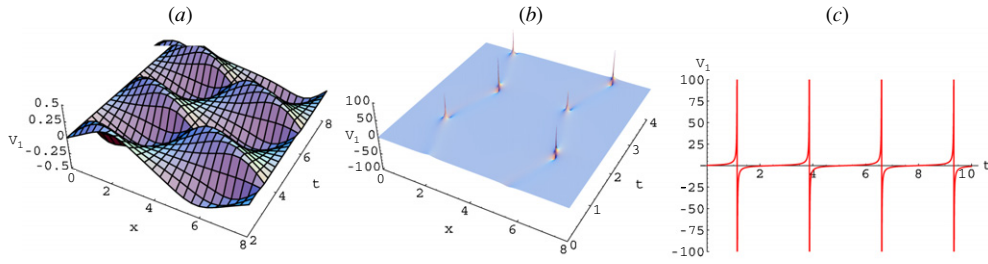


**Figure 5.** The spatiotemporal evolutions of flow velocity field  $v_1$  for  $V_c = 0.979E_R$  and (a)  $V_0 = 0.123E_R < V_c/3$ ,  $V_1 = \sqrt{2V_0(V_c - V_0)} \simeq 0.453E_R$ ,  $\beta = 0$ ; (b)  $V_0 = 0.823E_R > V_c/3$ ,  $V_1 = \sqrt{2V_0(V_c - V_0)} \simeq 0.506E_R$  and  $\beta = 5\pi/6$ . Part (c) is the projection of part (b) on the plane of  $v_1$  versus  $t$ . The flow velocity is in unit of  $10^{-2} \text{ m s}^{-1}$ ,  $x$  and  $t$  are normalized by  $10^{-7} \text{ m}$  and  $10^{-4} \text{ s}$ , respectively. The values of  $a_{s1}$ ,  $a_{s2}$ ,  $a_{s3}$  and  $N'_1$  are the same with figure 1(a). The blowing-up times are given by equation (34) as  $t_{b1} = (2l + \frac{5}{6})\frac{\pi}{\omega}$  for  $l = 0, 1, 2, \dots$ .

(This figure is in colour only in the electronic version)

We are interested in the physics of phase blowing-up in case 3. For simplicity and without loss of generality, we will consider the temporal evolution character of  $\Theta_{jx}(x, t)$  at a fixed spatial point  $x_{b\mu}$  and take the case  $G_1 V_1 > 0$  and the site  $x_{b1}$  as an example. Applying them to equations (11) and (27) yields

$$\Theta_{jx}(x_{b1}, t) = \frac{\pm G_j k \sqrt{(V_c - V_0)(3V_0 - V_c)} \sin(\omega t - \beta)}{2G_j(V_c - V_0)[1 - \cos(\omega t - \beta)]} = \pm \frac{k}{2} \sqrt{\frac{3V_0 - V_c}{V_c - V_0}} \cot \frac{\omega t - \beta}{2}. \quad (32)$$

The singularity at  $t_{b1}$  is obvious, since  $\sin[(\omega t_{b1} - \beta)/2] = 0$  results in

$$\lim_{t \rightarrow t_{b1}} \Theta_{jx}(x_{b1}, t) = \infty. \quad (33)$$

The similar results are obtained at other spacetime points of  $(x_{b\mu}, t_{b\nu})$ , that is  $\Theta_{jx}(x_{b\mu}, t_{b\mu}) = \infty$  for  $G_1 V_1 > 0$  and  $\mu = 1, 2$ ; and  $\Theta_{jx}(x_{b\mu}, t_{b\nu}) = \infty$  for  $G_1 V_1 < 0$  and  $\mu, \nu = 1, 2$ ,  $\mu \neq \nu$ . From the definition of  $t_{b\mu}$ , the blowing-up time reads

$$t_{b\mu}(l) = \frac{(2l + \mu - 1)\pi + \beta}{\omega}, \quad (34)$$

where  $\mu = 1, 2$  and  $l$  is an arbitrary integer. Clearly, from equation (34) we have the difference between the adjacent blowing-up times as  $t_{b\mu}(l+1) - t_{b\mu}(l) = 2\pi/\omega$ , which is just the period of the laser field.

Noticing the original definition  $\Theta_{jx}(x, t) = \lim_{\Delta x \rightarrow 0} \frac{\Delta \Theta_j}{\Delta x}$ , the infinite first derivative in equation (33) implies a jump of the phase,  $\lim_{\Delta x \rightarrow 0} \Delta \Theta_j(x_b, t_b) \neq 0$ , at the blowing-up spatiotemporal points. The phase jump is an important property of the phase blowing-up, which leads to the singularity of the velocity field. From equations (28) and (11), we plot the spatiotemporal evolutions of the velocity field  $v_1$  as in figure 5. In figure 5(a), we display that when the system parameters are taken in the region  $|V_1| > 2|V_0|$  of case 1, the velocity field  $v_1$  periodically evolves in time and coordinate without blowing-up. When the parameters are taken in the region  $|V_1| < 2|V_0|$  of case 3, the velocity field  $v_1$  periodically blows up as in figure 5(b). Figure 5(c) is the projection of figure 5(b) on the plane of  $v_1$  versus  $t$ , that clearly exhibits the periodic jumps of velocity field from  $|v_1(t_{b\mu})| = \infty$  to  $-|v_1(t_{b\mu})| = -\infty$  as the increase of time. The time interval of two adjacent blowing-ups is given by equation (34)

as  $\frac{2\pi}{\omega}$ , which is just the period of the laser field. During two jumps, the velocity field continuously evolves from  $-|v_1[t_{b\mu}(l)]|$  to zero, then to  $|v_1[t_{b\mu}(l+1)]|$ . The velocity field  $v_2$  has the similar properties, which are not shown in the figure.

It is interesting to see the behaviour of flow density  $\vec{J}_j(x, t)$  at the blowing-up time  $t_{b\mu}$ . The flow density in equation (28) is a simple sinusoidal function of time and obeys the relations  $J_j(x, t_{b\mu}) = 0$  and  $\vec{J}_j(x, t_{b\mu} + \varepsilon) = -\vec{J}_j(x, t_{b\mu} - \varepsilon)$  for  $|\varepsilon| \ll 1$ . These mean that the net current of BEC vanishes at any blowing-up time and the atomic current changes its direction when a blowing-up time is crossed. The inversion of flow vector implies that the BEC wave packet at any spatial site produces quantum reflections [31] at every blowing-up time  $t_{b\mu}$ , so the matter wave periodically oscillates with the laser frequency. The amplitude of flow density in equation (28) is proportional to the laser strength  $V_1$  and wave vector  $k$ . Therefore, we can control the atomic current by adjusting the frequency, wave vector and strength of the laser field.

#### 4. Conclusions and discussions

In summary, we have investigated a two-component BEC system confined in an optical lattice, by adding another spacetime periodic laser standing wave. Under the balance conditions between the internal and external potentials, we have constructed a set of EFSs. The balance region of parameter space is found and the time-space periodical atomic-number densities of the EFSs are illustrated. It is shown that the different atomic distributions correspond to different properties of the EFSs. Several important properties such as the atomic current, phase coherence and phase blowing-up, and the quantum reflection are investigated analytically and numerically. The bifurcation point for the phase blowing-up and the blowing-up region on the parameter space are given. We also find the spacetime singular points of velocity fields, which are the zero points of atomic-number densities. However, the zero points of the densities are not certainly the singular points of velocity field. Influences of the phase blowing-up to the velocity fields and flow densities are revealed. It is demonstrated that the velocity fields and flow densities periodically oscillate with frequency equating the laser frequency, and with wave vector and amplitude being proportional to the laser wave vector and strength. This supplies a scheme to control the BEC motions by adjusting the frequency, wave vector and strength of the laser field.

It should be pointed out that the phase blowing-up differs from the state blowing-up [24, 25], since the singular points of phase gradient just are the zero points of the module  $|\psi_j| = R_j$ . In other words, although the phase gradient may be an infinity at the spacetime point  $(x_{b\mu}, t_{bv})$ , the gradients  $\psi_{jx}(x_{b\mu}, t_{bv})$  and  $R_{jx}(x_{b\mu}, t_{bv})$  are finite. So we cannot determine whether the phase blowing-up causes the collapse of BEC although the blowing-up states are related to the collapses [25]. On the other hand, the phase blowing-up cannot directly affect the phase coherence of the EFSs, because of the zero module at the blowing-up spacetime points,  $R_j(x_{b\mu}, t_{bv}) = 0$ . It is worth to further study the relationships between the phase blowing-up and experimentally detectable properties, for example, the stability of EFSs and collapse of BEC.

#### Acknowledgments

This work was supported by the National Natural Science Foundation of China under Grant Nos 10575034 and 10275023, and by the Key Laboratory of Magnetic Resonance and Atomic and Molecular Physics of China under Grant No T152504.

## References

- [1] Dalfobo F, Giorgini S, Pitaevskii L P and Stringari S 1999 *Rev. Mod. Phys.* **71** 463
- [2] Pérez-García V M, Michinel H and Herrero H 1998 *Phys. Rev. A* **57** 3837
- [3] Kevrekidis P G and Frantzeskakis D J 2004 *Mod. Phys. Lett. B* **18** 173
- [4] Theodorakis S and Leontidis E 1997 *J. Phys. A: Math. Gen.* **30** 4835
- [5] Bronski J C, Carr L D, Deconinck B and Kutz J N 2000 *Phys. Rev. Lett.* **86** 1402
- [6] Deconinck B, Kutz J N, Patterson M S and Warner B W 2003 *J. Phys. A: Math. Gen.* **36** 5431
- [7] Hai W, Li Y, Xia B and Luo X 2005 *Europhys. Lett.* **71** 28
- [8] Deconinck B, Frigyyik B A and Kutz J N 2001 *Phys. Lett. A* **283** 177
- [9] Hai W, Chong G, Xie Q and Lu J 2004 *Eur. Phys. J. D* **28** 267
- [10] Kostov N A, Enol'skii V Z, Gerdjikov V S, Konotop V V and Salerno M 2004 *Phys. Rev. E* **70** 056617
- [11] Bronski J C, Carr L D, Deconinck B, Kutz J N and Promislow K 2001 *Phys. Rev. E* **63** 036612
- [12] Hai W, Lee C, Fang X and Gao K 2004 *Physica A* **335** 445
- [13] Liang Z X, Zhang Z D and Liu W M 2005 *Phys. Rev. Lett.* **94** 050402
- [14] Xue J 2005 *J. Phys. B: At. Mol. Opt. Phys.* **38** 3841
- [15] Bradley R M, Deconinck B and Kutz J N 2005 *J. Phys. A: Math. Gen.* **38** 1901
- [16] Vela-Arevalo Lu V and Fox R F 2005 *Phys. Rev. A* **71** 063403
- [17] Hur G, Creffield C E, Jones P H and Monteiro T S 2005 *Phys. Rev. A* **72** 013403
- [18] Zhang C, Nie Y and Liang J 2006 *Phys. Rev. B* **73** 085307
- [19] Villas-Bôas J M, Ulloa S E and Studart N 2004 *Phys. Rev. B* **70** 041302
- [20] Barash D and Orel A E 1999 *Phys. Rev. A* **61** 013402
- [21] André Eckardt, Weiss C and Holthaus M 2005 *Phys. Rev. Lett.* **95** 260404
- [22] Holthaus M 2001 *Phys. Rev. A* **64** 011601
- [23] Hensinger W K, Mouchet A, Julienne P S, Delande D, Heckenberg N R and Rubinsztein-Dunlop H 2004 *Phys. Rev. A* **70** 013408
- [24] Saito H and Ueda M 2001 *Phys. Rev. Lett.* **86** 1406
- [25] Konotop V V and Pacciani P 2005 *Phys. Rev. Lett.* **94** 240405
- [26] Gardiner S A, Jaksch D and Dum R 2000 *Phys. Rev. A* **62** 023612
- [27] Kevrekidis P G, Nistazakis H, Frantzeskakis D J, Malomed B A and Carretero-González R 2004 *Eur. Phys. J. D* **28** 181
- [28] Mason A, Portor, Kevrekidis P G and Malomed B A 2004 *Physica D: Nonlinear Phenom.* **196** 106
- [29] Inoué S, Andrews M R, Stenger J, Miesner H-J, Stamper-Kurn D M and Ketterle W 1998 *Nature* **392** 151
- [30] Guo B and Pang X 1987 *Solitons* (Beijing: Science Press) p 243 (in Chinese)
- [31] Lee C and Brand J 2006 *Europhys. Lett.* **73** 321